RSC Advances

ROYAL SOCIETY OF CHEMISTRY

www.rsc.org/advances

Conjugation of polyethylenimine and its derivatives to carbon-encapsulated iron nanoparticles

Artur Kasprzak,[a*] Magdalena Popławska,[a] Michał Bystrzejewski,[b] Olga Łabędź[b] and Ireneusz P. Grudziński[c]

[a] Faculty of Chemistry, Warsaw University of Technology, 00-664 Warsaw, Poland
[b] Faculty of Chemistry, University of Warsaw, 02-093 Warsaw, Poland
[c] Faculty of Pharmacy, Medical University of Warsaw, 02-097 Warsaw, Poland

Abstract

Carbon-based nanomaterials functionalized by cationic polymers are interesting starting materials for the development of the nanotheranostic systems. In this study, the polyethylenimine (PEI) and its pre-synthesized derivatives, were conjugated to carbon-encapsulated iron nanoparticles (CEINs). Branched PEIs of various molecular weight were derivatized. The aim of the polymer modification was to introduce the carboxylic functionality to the PEI structure. Two different synthetic pathways were proposed: the amide-type reaction with the succinic acid anhydride and the reductive amination using the *p*-formylbenzoic acid. The polyethylenimine derivatives were analyzed by means of spectroscopic methods (NMR, FT-IR). In order to determine the ratio of primary, secondary and tertiary amine groups in modified polymers, the inverted-gate ^{13}C NMR spectroscopy was applied. Next, CEINs modified with two different surface carboxylic linkers were functionalized using pristine PEIs and their derivatives. The conjugation of the polymer to the surface-modified nanoparticles was carried out using carbodiimide-amine type reaction. The success of the conjugation process was confirmed by thermogravimetry and infrared spectroscopy. The morphological details were analyzed using transmission electron microscope, whilst surface zeta potential and the average particle size were determined by dynamic light scattering. It was found that the molecular weight of the polymer and the type of the surface linker were the key factors which crucially influenced the functionalization yield and the physiochemical features of the synthesized nanoplatforms. The best dispersion

* Corresponding author: E-mail: akasprzak@beryl.ch.pw.edu.pl (Artur Kasprzak)

stability in the aqueous media and the smallest mean hydrodynamic particle size was found for CEINs with the longer carboxylic linker.

keywords: polyethylenimine; carbon-encapsulated iron nanoparticles; nanomaterials; conjugation; nanomedicine; theranostics.

1. Introduction

The treatment of serious diseases, such as cancer, in most cases is associated with aggressive and a patient-unfriendly therapy. Most for antineoplastic agents especially those of alkylating compounds, antimetabolites, natural products of Vinca alkaloids, epipodophyllotoxins and some miscellaneous chemicals, widely used in modern anti-cancer therapies, have a very low or narrow therapeutic index.[1-3] In preclinical studies of such drugs it means that a median lethal dose (LD_{50}) of the drug is nearly the same as a median effective pharmacological dose (ED_{50}) of this medicine. Each chemotherapy of the tumor, if feasible, involves also a number of undesirable or adverse toxic events to patients. In other words, adverse reactions are a cost of modern anticancer therapy. Therefore, the anticipated benefit from any therapeutic decision must be balanced by the potential risk. Hence, there is an urgent need to develop and apply new methods of the cancer treatment using nanomaterials possessing both early diagnostic and therapeutic features. An interesting and a promising method is creating the multifunctional theranostic system, which allows to personalize the anticancer therapy in humans.[4-6]

The development of the nanotechnology caused the growing interest of this field of science in terms of the biomedical application of different nanomaterials. So far, many articles on application of nanostructures in the theranostic platforms have been published.[7-12] Mura and Couvreur called those smart and versatile platforms 'nanotheranostics'.[13] Such nanostructures are constructed of the four main building units including: (i) the nanostructure 'core', used as a nanocarrier and diagnostic contrast agent (most commonly for in MR imaging), (ii) a drug carrier or a gene delivery non-biologic vector, i.e. cationic polymer, (iii) a targeting ligand, like peptide, protein, aptamer or antibody, which recognizes and selectively binds into the molecular target (i.e nuclear receptors in the tumor), and (iv) a therapeutic unit such as drugs, nucleic acids, protein, enzymes etc. In the first step of the nanotheranostic platform synthesis, most frequently, the nanomaterial-polymer

conjugate is created. The concept of the building units is up to a further strategy to be used in anticancer therapy, but there are nanostructures and macromolecules, that ceaselessly attract a great deal of attention, due to potential application in the future human nanomedicine.

Carbon-based nanomaterials exhibit extraordinary features related to their size and physical properties.[14-16] It was found that this group of materials is one of the best nanocarriers recently examined in preclinical anticancer studies and modern diagnostic. In particular, noteworthy are metal-cored carbon structures, which besides the above applications, constitute the contrast-like agents, so they can be used, i.e. in magnetic resonance imaging (MRI). Undeniably, such magnetic nanomaterials are very interesting proposal for building the units of the nanotheranostic 'core'. For example, Bosi *et al*. showed that gadolinium (strongly paramagnetic metal widely used in MR imaging) could be permanently locked into the C_{60} fullerene cage.[17] Note that the toxicity of gadolinium in this kind of structures, called 'metallofullerenes', is reduced in comparison to currently used positive contrast agents (i.e. Magnevist®). Carbon-encapsulated iron nanoparticles (CEINs), synthesized in our laboratory, exhibit even more interesting and promising shape- and size-depended properties.[18-20] This kind of encapsulates (the core-shell type nanomaterial), are built of the spherical-shape iron core and the tight carbon (graphene-like) coating of high chemical inertness. The carbon-encapsulation method is employed to retain the inherent magnetic properties of these nanomaterial, by protecting against adverse environmental factors and possible agglomeration and/or aggregation in different media including human fluids. Hence, the CEINs platforms could be considered as a potential theranostic nanomaterial addressing to the molecular diagnostic (mMRI) and therapy of cancers. Note that our previous research showed the cytotoxic effects of these magnetic nanoparticles on human and murine melanoma[21] as well as lung carcinoma cells (in vitro).[22]

An interesting feature of carbon nanomaterials is the ability to adsorb or covalent binding of macromolecules, i.e. polymers,[23] biomolecules,[24] and target drugs.[25,26] The surface modification of nanomaterials (introducing functionalities) is being widely studied, due to the further possibility of the covalent-type functionalization using various macromolecules. So far, many ways of introducing such functional groups (most commonly carboxylic functionalities) were proposed, for fullerenes,[17] nanotubes,[27,28] and graphene.[29,30] Also, the introduction of such surface functionalities onto carbon-encapsulated iron nanoparticles were recently reported in our studies.[31,32]

After nanomaterial selection for the pre-nanotheranostic platform, a real challenge is the choice of the most appropriate and promising therapeutic-unit carrier. This kind of

non-biological vector should provide the adequate drug/gene delivery and the stabilization of the transferred therapeutic medicine under *in vivo* conditions.

Cationic polymers, i.e. chitosan and dextran, are widely studied due to their interesting features and therapeutic potential.[33-35] It was found, that this group of macromolecules showed encouraging abilities in the delivering of nucleic acids (i.e. siRNA),[36,37] and drugs.[38,39] Polyethylenimine (PEI) is one of the most interesting cationic polymer, which has all the required biomedical-field features and is widely used as the building unit in the nanomaterial-polymer conjugates. To date, a variety of PEI-carbon material conjugates were proposed, i.e. using nanotubes,[40-42] and graphene.[43-45] The aim of the synthesis of such hybrids is to improve: (i) the solubility of the nanoplatform in aqueous/buffer media, (ii) the stability under the physiological conditions and (iii) the terapeutic efficiency. One has to be noted that the cytotoxicity and toxicity of PEI is related to the molecular weight of this polymer: the cytotoxic potential (as well as toxicity) increases with the molecular weight. For example, Feng at al. showed that cytotoxity of PEI to HeLa cells (cervical cancer cell line) is associated with the molecular weight of the adsorbed polymer.[46] For PEI concentration of 300 mg/L, the relative viability of HeLa cells for PEI 1.2kDa was found to be approximately 90%, whilst only 20%was noted using PEI 10kDa, respectively. Moreover, it was shown, that creating such covalent or non-covalent carbon nanomaterial-PEI conjugates, decreases the systemic toxicity of polyethylenimine. A proper balance to be established between toxicity and pharmacological efficacy of the polymer used as a drug delivery system and/or gene transfer carrier is the main point and challenge in creating such nanotheranostics for the modern anticancer therapy.

Since the first investigation into polyethylenimine's application in biomedical field, many publications on the surface chemical modification of this polymer have been reported. Some of authors showed versatile and an effective synthetic strategies of PEI derivatives, i.e. acylation,[47,48] or introducing hydrophobic substituents.[49,50] Also, more complex hybrid polymer structures were proposed, including chitosan-PEI copolymers,[51] dextran-PEI polycationic vectors,[52] and pullulan-PEI-folic acid conjugates.[53] Most commonly, the biocompatibility of polyethylenimine is improved, by grafting PEI with poly(ethylene glycol) (PEG).[54,55] These results suggest the very important fact, that PEI modifications result in the reduction of the polymer toxicity, as well as increase of the drug delivery or gene transfection efficiency in biological systems. However, both of these features are heavily dependent on the molecular weight of the used polyethylenimine. Undeniably also, PEI derivatives decorated with the specific functionalities (i.e. carboxylic or sulfhydryl groups)

allow for further conjugation-type reactions. In terms of the nanotheranostic synthesis these functionalities constitute incredibly important starting points (chemical targets) for structural-expansion of the pre-theranostic wireframe.

In this work, we have undertaken an attempt to synthesize the basic wireframe of the nanotheranostic system consisting carbon-encapsulated iron nanoparticles and polyethylenimine. The biomedical potential of the PEI nanoconstruct prompted us, to try answer the fundamental question on the possibility of the conjugation-type reaction between surface-modified CEINs with pristine PEI and pre-synthesized PEI derivatives.

2. Experimental section

2.1 Materials and instrumentation

Carbon-encapsulated iron nanoparticles were synthesized using the so-called carbon arc route. The nanoparticles synthesis strategy and linker surface-modification were described elsewhere.[31] The arc plasma synthesis yielded core-shell iron-carbon nanoparticles, which after purification comprise of magnetic encapsulates with the diameter between 10 and 100 nm. The introduction of carboxylic functionalities onto CEINs surface is based on two strategies: sonicating of the pristine nanomaterial in H_2SO_4/HNO_3 mixture, or via radical-type reaction with succinic acid acyl peroxide. Both modification strategies cause a partial degradation of the carbon coating. Hereafter, the raw products are referred as Fe@C (pristine CEINs), Fe@C-COOH (shorter linker) and Fe@C-$(CH_2)_2$-COOH (longer linker). The carboxylic moieties content on the surface of modified CEINs is 0.53 mmol·g^{-1} and 1.42 mmol·g^{-1}, for Fe@C-COOH and Fe@C-$(CH_2)_2$-COOH, respectively.[31]

Branched polyethylenimine of various molecular weight (PEI; M_w (by LS): 0.8 kDa, 25 kDa, 750 kDa), succinic acid anhydride (SAA), *p*-formylbenzoic acid (pFBA), sodium borohydride, *N*-(3-dimethylaminopropyl)-*N'*-ethylcarbodiimide hydrochloride (EDCl), *N*-hydroxysulfosuccinimide (NHS) were purchased from Sigma-Aldrich and were used as received without purification.

Thermogravimetric analysis (TGA) was performed with TA Q-50 instrument under nitrogen (heating rate: 5 °C/min) atmosphere. The morphology was analyzed by transmission electron microscopy (TEM) using Zeiss Libra Plus instrument (accelerating voltage: 120 kV). Dynamic light scattering (DLS) and the zeta potential measurements were performed using

Malvern Zetasizer instrument. The measurements were conducted on the nanomaterial samples suspended in distilled water (100 $\mu g \cdot ml^{-1}$).

Fourier transformation infrared (FT-IR) spectra were recorded in a transmission mode with Thermo Scientific Nicolet iS5 spectrometer with a resolution of 8 cm^{-1}. The samples were analyzed as pellets with dry KBr, whilst PEI and its derivatives were applied as thin film onto a pellet made of pure KBr. ^{1}H NMR and ^{13}C NMR spectra were recorded on a Varian NMR System spectrometer (500MHz, 125MHz) or Varian Gemini 2000 spectrometer (200MHz, 50 MHz), in deuterium oxide. MestRe-C 2.0 software was used for NMR spectra simulation (*MestRe-C NMR Data Processing Made Easy 4.9.9.6, 1996– 2006, courtesy F.J. Sardina, Universidad de Santiago de Compostela, Spain*).

Sonication of carbon materials was performed using Bandelin Sonorex RK 100 H ultrasonic probe (ultrasonic peak output/HF power: 320W/80W; 35 kHz). The as-obtained suspensions were centrifuged on MPW-260R centrifuge (5000RPM, 24 °C).

The dialysis against water was carried out using 10k MCWO Snake-Skin® Dialysis Tubes (Thermo-Fisher Scientific). The lyophilisation was performed with FreeZone 1 liter Laboratory Lyophilizer (LABCONCO).

2.2 Synthesis of PEI-SA

PEI-SA derivatives were synthesized using modified the methods described elsewhere.[54,56] The reaction scheme is shown in **Fig. 1** (route **a)**. First, the solution of 500 mg PEI (0.8 kDa, 25 kDa or 750 kDa) in 10 ml of distilled water was prepared. Then, 33 mg (0.33 mmol) of succinic acid anhydride was dissolved in 5 ml of DMSO and slowly added dropwise into the vigorously stirred PEI solution. The mixture was then stirred at room temperature for 24 h and then the obtained turbid-white mixture was dialyzed (10k MWCO membrane) against distilled water for 48 h. Finally, product was lyophilized for 24 h. Average reaction yield was ca. 57%. Due to the membrane pore size, PEI0.8k-SA derivative was not dialyzed, and used in further research without purification.

PEI0.8k-SA: ^{1}H NMR δ_H (200MHz, D_2O, ppm): 2.40 (bs, 4H, -C_2**H_4**-COOH), 2.50-2.74 (bm, PEI), 2.93-2.94 (bm, PEI), 3.23-3.30 (bm, 2H, {PEI}-C**H_2**-NH-CO-),
^{13}C NMR δ_c (50MHz, D_2O, ppm): 32.73 ({PEI}-NH-CO-**C**H_2-), 33.41 (-**C**H_2-COOH), 37.94 (PEI), 39.95 (PEI), 45.75 (PEI), 47.76 (PEI), 50.47 (PEI), 50.61 (PEI), 51.20 (PEI), 53.22 (PEI), 55.84 (PEI), 175.84 ({PEI}-NH-**C**O-), 180.74 (-**C**OOH)

PEI25k-SA: **^{1}H NMR** δ_H (500MHz, D_2O, ppm): 2.45 (bs, 4H, -C_2**H_4**-COOH), 2.66-2.80 (bm, PEI), 3.14-3.15 (bm, PEI), 3.29-3.32 (bm, 2H, {PEI}-C**H_2**-NH-CO-)

FT-IR υ (film, cm^{-1}): 1645 (C=O ; amide I)

PEI750k-SA: **^{1}H NMR** δ_H (500MHz, D_2O, ppm): 2.56 (bs, 4H, -C_2**H_4**-COOH), 2.77-2.92 (bm, PEI), 3.24-3.28 (bm, PEI), 3.41-3.44 (bm, 2H, {PEI}-C**H_2**-NH-CO-)

2.3 Synthesis of PEI-pFBA

PEI-pFBA derivatives were synthesized using the reductive amination approach. The reaction scheme is shown in **Fig. 1** (route **b**). To the stirred solution of 500 mg PEI (0.8 kDa, 25 kDa or 750 kDa) in 10 ml of dried methanol, 37.5 mg (0.25 mmol) of *p*-formylbenzoic acid was added in one portion. The mixture was refluxed under argon atmosphere for 1 h and then stirred at room temperature for 24 h. Sequentially, 38.0 mg (1.0 mmol) of sodium borohydride was added. The reaction mixture was stirred for 4 h at room temperature and then solvent was evaporated using a rotary evaporator. The as-obtained bright-yellow residue was dissolved in 5 ml of distilled water and extracted three times with 7 ml of ethyl acetate. The aqueous phase was dialyzed (10k MWCO membrane) against distilled water for 48 h. The obtained product was lyophilized for 24 h. Average reaction yield was ca. 50%. Once again, PEI0.8k-pFBA derivative was not dialyzed, and used in conjugation reactions with CEINs without further purification.

PEI0.8k-pFBA: **^{1}H NMR** δ_H (200MHz, D_2O, ppm): 2.60-2.64 (bm, PEI), 2.97-2.98 (bm, PEI), 3.27-3.29 (bm, 2H, {PEI}-C**H_2**-NH-CH_2-C_6H_4-), 3.74 (bs, 2H, {PEI}-NH-C**H_2**-C_6H_4-), 7.34-7.38 (bm, 2H, -NH-CH_2-C_6**H_4**-), 7.78-7.84 (bm, 2H, -C_6**H_4**-COOH)

^{13}C NMR δ_C (125MHz, D_2O, ppm): 38.04 (PEI), 39.89 (PEI), 46.01 (PEI), 47.92 (PEI), 49.09 (PEI), 50.04 (PEI), 51.40 (PEI), 53.24 (PEI), 55.03 (PEI), 128.79 (-**C**$_6H_4$-COOH), 129.82 (-NH-CH_2-**C**$_6H_4$-), 136.07 ({PEI}-NH-**C**H_2-C_6H_4-), 142.50 ({PEI}-NH-CH_2-**C**$_6H_4$-), 164.85 (-**C**$_6H_4$-COOH), 174.61 (-**C**OOH)

PEI25k-pFBA **^{1}H NMR** δ_H (500MHz, D_2O, ppm): 2.61-2.77 (bm, PEI), 3.03-3.11 (bm, PEI), 3.25-3.30 (bm, 2H, {PEI}-C**H_2**-NH-CH_2-C_6H_4-), 3.76 (bs, 2H, {PEI}-NH-C**H_2**-C_6H_4-), 7.34-7.39 (bm, 2H, -NH-CH_2-C_6**H_4**-), 7.85-7.93 (bm, 2H, -C_6**H_4**-COOH)

FT-IR υ (film, cm^{-1}): 760 (C-H), 1370 (C=C), 1600 (C=O)

PEI750k-pFBA: **^{1}H NMR** δ_H (500MHz, D_2O, ppm): 2.65-2.86 (bm, PEI), 3.10-3.15 (bm, PEI), 3.28-3.32 (bm, 2H, {PEI}-C**H_2**-NH-CH_2-C_6H_4-), 3.80 (bs, 2H, {PEI}-NH-C**H_2**-C_6H_4-), 7.40-7.43 (bm, 2H, -NH-CH_2-C_6**H_4**-), 7.85-7.88 (bm, 2H, -C_6**H_4**-COOH)

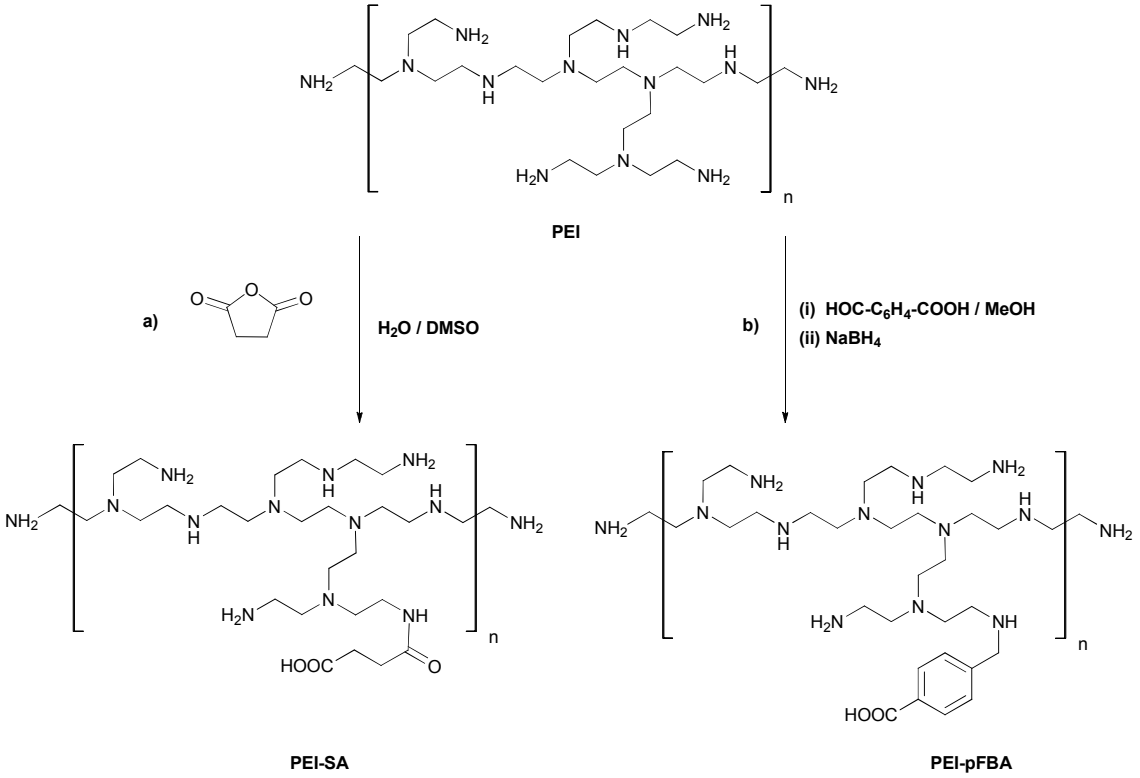

Fig. 1. The synthesis of PEI derivatives: **a**) PEI-SA, **b**) PEI-pFBA

2.4 Conjugation of pristine PEI to surface-modified CEINs

The reaction scheme is shown in **Fig. 2**. 20 mg of Fe@C-COOH or Fe@C-$(CH_2)_2$-COOH, *N*-(3-dimethylaminopropyl)-*N*'-ethylcarbodiimide hydrochloride (EDCl) (10 mol equivalent per 1 mol COOH groups) and *N*-hydroxysulfosuccinimide (NHS) (25 mol equivalent per 1 mol COOH groups) were sonicated in 10 ml of distilled water, for 1 h. Then, 200 mg of PEI (0.8 kDa, 25 kDa or 750 kDa) in 10 ml of distilled water was added to the carbon material suspension and sonicated for 5 h at room temperature. Afterwards, the obtained conjugate suspension was centrifuged several times (5000RPM, 24 °C, 25 min) in methanol. The PEI content in the following supernatants was monitored by TLC (a ninhydrin test was used). Finally, the carbon material was dried at 45 °C for 24 h. The observed positive mass gain pre-indicated the success of the conjugation. Due to the highly hygroscopic features of this kind of nanomaterial-polymer conjugate, the observed mass gain could not be directly taken as the real conjugation yield.

The obtained products were named as NANO-1.1-1.3 and NANO-2.1-2.3 for Fe@C-CONH-PEI and Fe@C-$(CH_2)_2$-CONH-PEI, respectively.

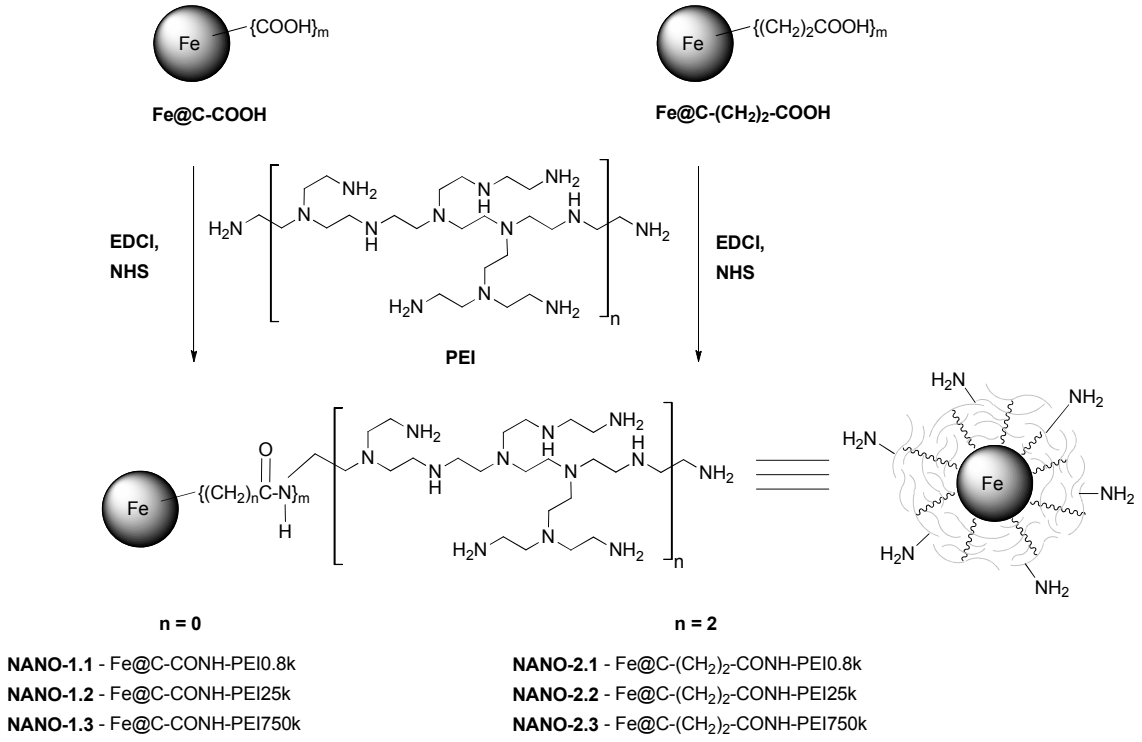

Fig. 2. Conjugation of pristine PEI to carbon-encapsulated iron nanoparticles

2.5 Conjugation of PEI-SA and PEI-pFBA to surface-modified CEINs

The reaction scheme is shown in **Fig. 3**. Prior to the conjugation 20 mg of Fe@C-COOH or Fe@C-$(CH_2)_2$-COOH, *N*-(3-dimethylaminopropyl)-*N*'-ethylcarbodiimide hydrochloride (EDCl) (10 mol equivalent per 1 mol COOH groups) and *N*-hydroxysulfosuccinimide (NHS) (25 mol equivalent per 1 mol COOH groups) were sonicated in 10 ml of distilled water, for 3 h. Then, the supernatant was precisely separated from the nanoparticles and removed from the flask using Pasteur pipette (carbon-encapsulated iron nanoparticles were immobilized using a magnet). Next, to the carbon material residue, a solution 200 mg of appropriate PEI derivative (PEI-SA or PEI-pFBA) in 10 ml of distilled water, was added. The sonication was performed for 4 h at room temperature. The obtained suspension was centrifuged several times (5000RPM, 24 °C, 30 min) with methanol, until the polymer was not present in a supernatant (a ninhydrin test was used). The final carbon material was dried at 45 °C for 24 h.

The obtained products were named as NANO-3.1-3.3, NANO-4.1-4.3, NANO-5.1-5.3 and NANO-6.1-6.3 for Fe@C-CONH-PEI-SA, Fe@C-$(CH_2)_2$-CONH-PEI-SA, Fe@C-CONH-PEI-pFBA and Fe@C-$(CH_2)_2$-CONH-PEI-pFBA, respectively.

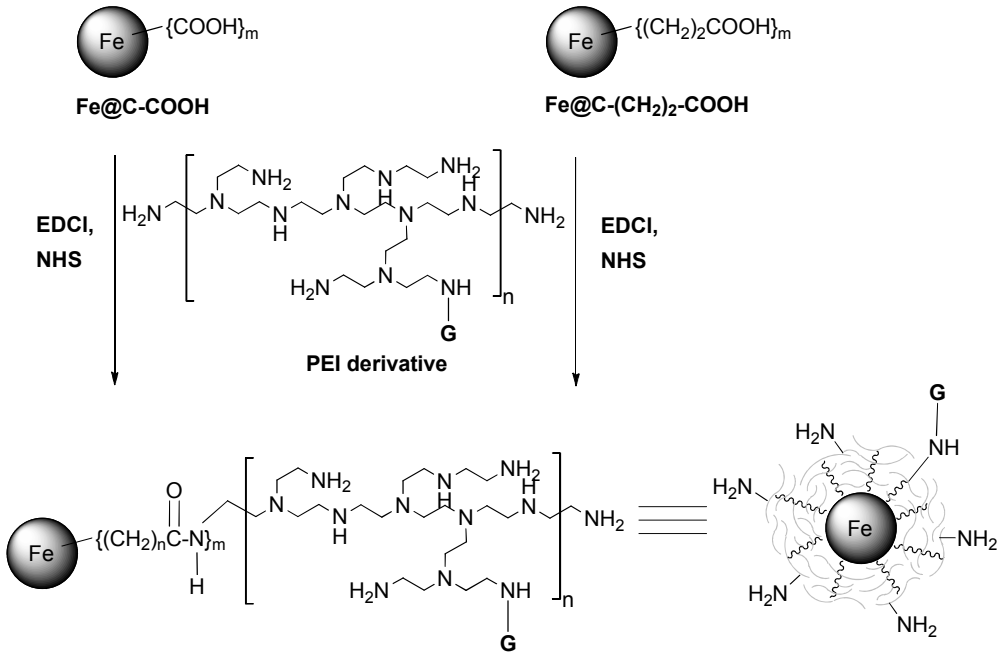

NANO-3.1 - Fe@C-CONH-PEI0.8k-SA
NANO-3.2 - Fe@C-CONH-PEI25k-SA
NANO-3.3 - Fe@C-CONH-PEI750k-SA

NANO-4.1 - Fe@C-$(CH_2)_2$-CONH-PEI0.8k-SA
NANO-4.2 - Fe@C-$(CH_2)_2$-CONH-PEI25k-SA
NANO-4.3 - Fe@C-$(CH_2)_2$-CONH-PEI750k-SA

G = $CH_2C_6H_4COOH$ (PEI-pFBA)

NANO-5.1 - Fe@C-CONH-PEI0.8k-pFBA
NANO-5.2 - Fe@C-CONH-PEI25k-pFBA
NANO-5.3 - Fe@C-CONH-PEI750k-pFBA

G = $CH_2C_6H_4COOH$ (PEI-pFBA)

NANO-6.1 - Fe@C-$(CH_2)_2$-CONH-PEI0.8k-pFBA
NANO-6.2 - Fe@C-$(CH_2)_2$-CONH-PEI25k-pFBA
NANO-6.3 - Fe@C-$(CH_2)_2$-CONH-PEI750k-pFBA

Fig. 3. Conjugation of PEI derivatives (PEI-SA and PEI-pFBA) to carbon-encapsulated iron nanoparticles

3. Results and discussion

3.1 Structural modification of PEI (synthesis of PEI-SA and PEI-pFBA)

The analysis of synthesized PEI derivatives was carried out using spectroscopic methods. First, ^{1}H and ^{13}C NMR spectra of products were recorded. The ^{1}H NMR spectra of: succinated PEI 25kDa (PEI25k-SA) and *p*-carboxybenzylated PEI 25kDa (PEI25k-pFBA) are shown in **Figs. 4** and **5**, respectively (other ^{1}H and ^{13}C NMR spectra of PEI derivatives are presented in Fig S2, Supplementary Data). There were no significant signal shifts of these derivatives in comparison the pristine PEI (^{1}H and ^{13}C NMR spectra of pristine PEI, please

see spectra 1-4 in Fig. S1 in Supplementary Data). The spectra of all products consist of the peaks corresponding to protons of PEI 25kDa and some new features that could be assigned to the introduced substituents. On the PEI25k-SA spectrum (**Fig. 4**) the signal from methylene groups of succinic acid is present (2.45 ppm), but a more significant broad multiplet is located at 3.29-3.32 ppm. This signal corresponds to the methylene moiety at the primary amine group of PEI with introduced succinic substituent ({PEI}-C**H$_2$**-NH-CO-(CH$_2$)$_2$-COOH). Please note, that 2.45 ppm and 3.29-3.32 ppm signal ratio is about 2:1, and this finding confirms our supposition about peak assignment and the success of PEI modification. The characteristic signals of the aromatic-ring protons are present (7.34-7.39 ppm and 7.85-7.93 ppm) for the PEI25k-pFBA sample (**Fig. 5**). The peak located at 3.79 ppm corresponds to the benzyl moiety ({PEI}-NH-C**H$_2$**-C$_6$H$_4$-), whilst the broad multiplet at 3.25-3.30 ppm is assigned to the methylene moiety at the primary amine group of PEI with introduced *p*-carboxybenzyl substituent ({PEI}-C**H$_2$**-NH-CH$_2$-C$_6$H$_4$-COOH). The peak ratio confirms the successful modification of PEI. Moreover, it is worth to note, that the peaks from substratum (succinic acid anhydride or *p*-formylbenzoic acid) and their analogs (i.e. *p*-carboxybenzyl alcohol, due to the possible reduction of the substrate) are not observed.

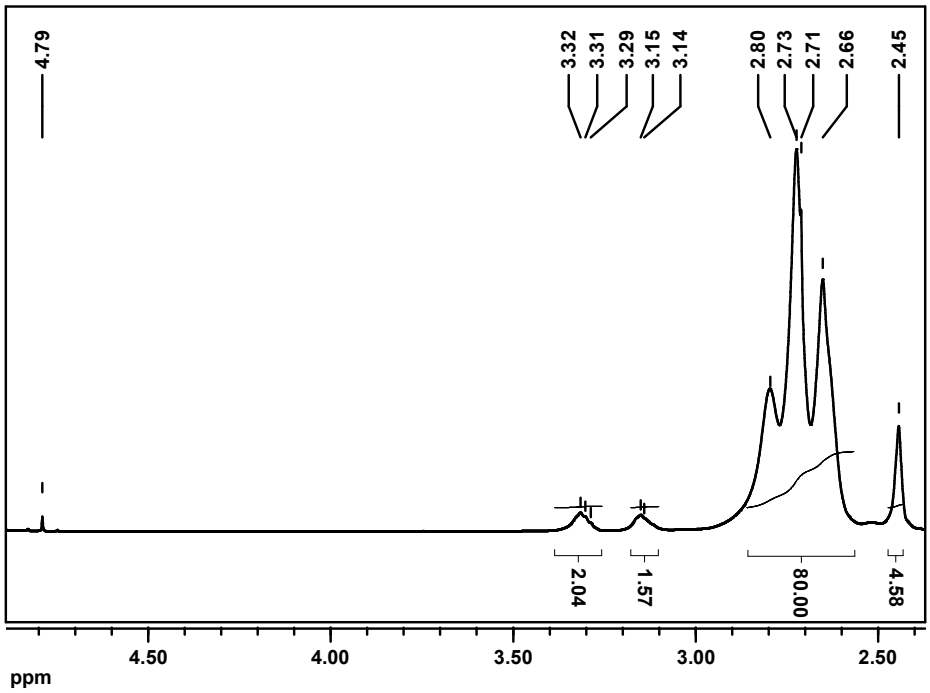

Fig. 4. ^{1}H NMR spectra of PEI25k-SA

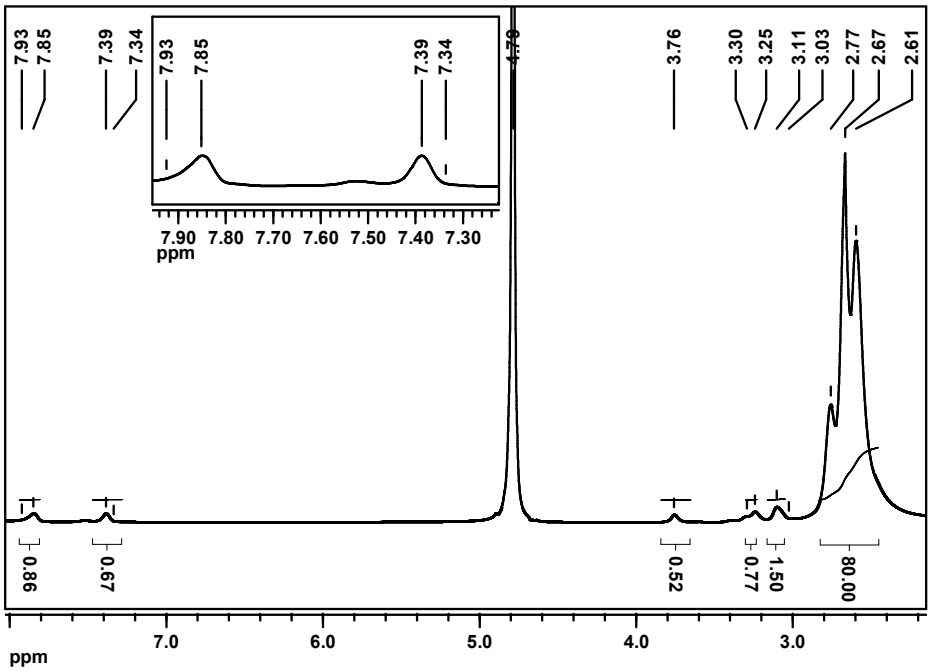

Fig. 5. ^{1}H NMR spectra of PEI25k-pFBA

Fourier transformation infrared (FT-IR) spectroscopy was finally carried out to confirm the success of each modification. **Fig. 6** shows the FT-IR spectra of pristine PEIs of various molecular weight. As it can be seen, the spectra are very similar. The bands at the lowest wavelengths corresponds to N-H stretching vibrations (3300-3450 cm^{-1}) and aliphatic C-H stretching vibrations (2810-2930 cm^{-1}). Incredibly important two strong bands are located at 1580 cm^{-1} and 1460 cm^{-1}, which are associated with the N-H vibrations of 1° and 2° amino groups, respectively. The band at 1460 cm^{-1} also correspond to the CH_2 moiety. The peaks at 1300 cm^{-1} and from the range 1040-1120 cm^{-1} corresponds to the C-N stretching vibrations. In **Fig. 7** we present spectra of two PEI derivatives: succinated PEI 25kDa (PEI25k-SA) and *p*-carboxybenzylated PEI 25kDa (PEI25k-pFBA) (for PEI 0.8kDa and 750kDa derivatives – data not shown). The bands which are typical for the pristine PEI appear on the spectrum of each derivative. For PEI25k-SA derivative, the new absorption band at 1645 cm^{-1} can be clearly assigned to the imposition of the amide I band and the stretching C=O vibration. In contrast, for PEI25k-pFBA derivative, the new absorption band is located at 1600 cm^{-1}. This feature can be attributed to the stretching vibrations of C=O moiety, as the result of the intramolecular interactions between the Ar-COOH substituent and amino groups of PEI. Due to those electrostatic interactions the position of the considered absorption band is downshifted in comparison to smaller molecules, e.g. benzoic acid. Moreover, for PEI25k-pFBA derivative the evident intensity enhancement is seen for bands located at 1370 cm^{-1} and 760 cm^{-1}, which could be assigned to the C=C skeletal vibration inside the aromatic ring and C-H out-of-plane ring vibrations, respectively.

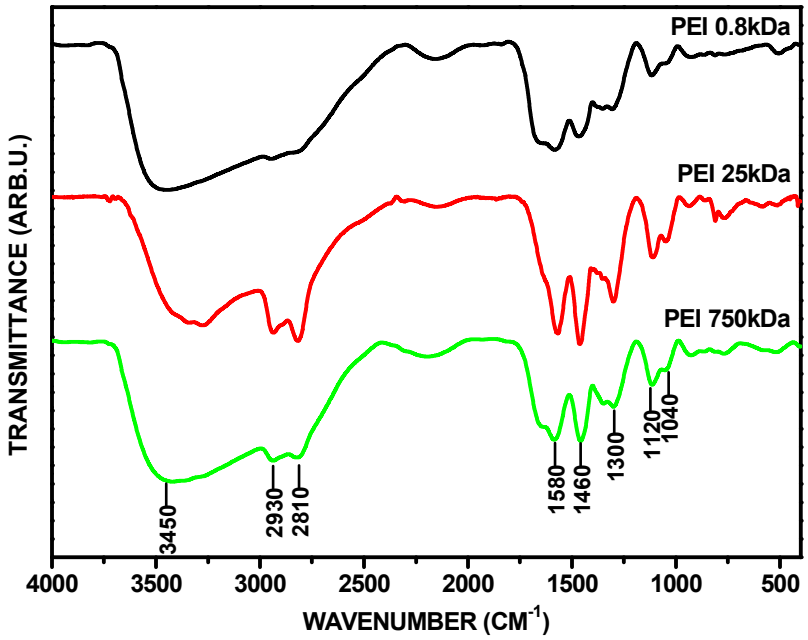

Fig. 6. FT-IR spectra of pristine PEIs

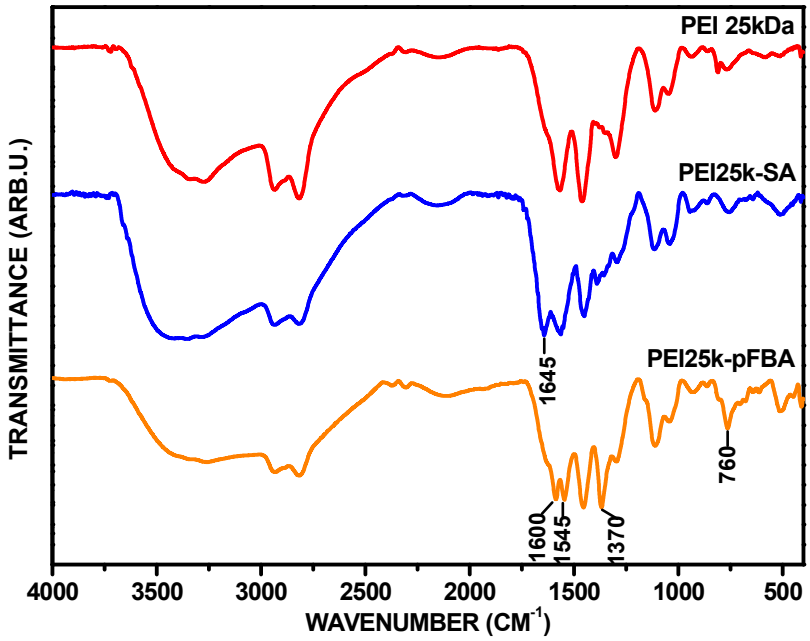

Fig. 7. FT-IR spectra of PEI 25kDa derivatives

In order to evaluate the PEI modification degree, the inverted-gate ^{13}C NMR spectroscopy was applied. The signals on the spectra were assigned as it was reported earlier.[57,58] Thus, PEI 25kDa and its derivatives were chosen as the representative polymer samples. We have found, that the ratio of primary, secondary and tertiary amine groups of pristine PEI 25kDa (NH_2 : NH : N) is 1 : 1,12 : 0.89 (please see spectrum 1 in Fig. S3 in Supplementary Data), whereas, this ratio for the polymer derivatives was quite different and equaled 1 : 1.62 : 1.32 and 1 : 1.69 : 1.39, for PEI25k-SA and PEI25k-pFBA, respectively (please see spectrum 2 and 3 in Fig. S3 in Supplementary Data). The ratio has changed quite significantly, with the reduction in the number of primary amino groups in synthesized polymer derivatives. Also, it could be calculated, that modification degree is about 10% (9.5% and 10.5% for PEI25k-SA and PEI25k-pFBA, respectively). Those observations proves that modifications of PEI were successful and indicate the similar degree of modifications of the polymer using succinic acid anhydride and *p*-formylbenzoic acid.

In most cases, the toxicity of PEI is explained by the high positive charge of PEI (and so high zeta potential).[47,59] Hence, the representative polymers: PEI 25kDa, PEI25k-SA and PEI25k-pFBA, were sonicated in water (100 $\mu g \cdot ml^{-1}$) and zeta potential (ZP) measurements were carried out. Firstly, PEI 25kDa was dialyzed against water for 48 hours, then the obtained fractions (remaining in the dialysis tube and the water fraction after dialysis) were evaporated under reduced pressure and lyophilized. As expected, the zeta potential (ZP) of each fraction was found to be +23.2 mV, +29.0 mV and +19.0 mV for pristine PEI (without dialysis), PEI fraction >10 kDa and PEI fraction <10 kDa, respectively. Sequentially, the zeta potential of PEI 25kDa derivatives was measured, and was found to be +21.0 mV and +28.7 mV, for PEI25k-SA and PEI25k-pFBA, respectively. Please note, that zeta potential of the polymer derivatives should be compared with ZP of PEI fraction >10 kDa, because the obtained products were dialyzed. Hence, the ZP of PEI derivatives, in comparison to pristine PEI 25kDa (fraction >10 kDa), is 1.31 and 1.01 fold lower, for PEI25k-SA and PEI25k-pFBA, respectively. This finding shows, that the succination and the *p*-carboxybenzylation of PEI results in the reduction of the zeta potential of PEI (especially for PEI-SA derivatives) due to the decreasing amount of available amino moieties in the polymer structure. If so, one has to consider the reduction of toxicity of PEI by synthesizing its carboxylic derivatives, combined with no significant decrease in binding capacity of biomolecules.

3.2 Synthesis and characterization of PEI-CEINs conjugates

The synthesis of polymer conjugates was performed with the carbodiimide-amine type reaction (EDCl, NHS). First, the results of the conjugation of PEI and its derivatives with carbon-encapsulated iron nanoparticles were analyzed qualitatively. FT-IR spectroscopy is the convenient technique for the analysis of the carbon materials and its conjugates with polymers. This technique in many cases allows to determine whether the conjugation reaction proceeded successfully. In **Fig. 8** we present two representative FT-IR spectra of conjugates: **a)** Fe@C-CONH-PEI (NANO-1.1-1.3) and **b)** Fe@C-$(CH_2)_2$-CONH-PEI-pFBA (NANO-6.1-6.3) (for other FT-IR spectra, please see spectra 1-4 in Fig. S4 in Supplementary Data). For comparison, the spectra of surface-functionalized CEINs are also shown. The bands which are characteristic for PEI appear on the spectrum of each conjugate, which means that the functionalization of CEINs was successful (please compare with PEIs spectra in **Fig. 6**). Moreover, in contrast to the pristine Fe@C-$(CH_2)_n$-COOH (n= 0 or 2) spectra, the band located at 1710 cm^{-1}, coming from C=O vibration in the carboxylic groups, is absent after the conjugation. It means, that nearly all carboxylic functionalities on the surface of CEINs participated in the formation of covalent amide bonds (in other words the CEINs conjugated to PEIs do not contain free-carboxylic groups). Also, the presence of PEI in the carbon materials can be confirmed by two weak bands founded at the lowest wavelengths (please see Fig. S5 in Supplementary Data). Those features located at 2850 cm^{-1} and 2925 cm^{-1} can be assigned to C-H stretching vibrations in CH_2 moieties of PEI, which were clearly visible in pristine PEIs spectra. Hence, it can be considered, that all conjugation reactions were successful. Please note, that due to the highly hygroscopic character of the obtained conjugates, the broad bands located on the spectrum beyond c.a. 2950 cm^{-1} cannot be directly assigned to N-H stretching vibrations of PEI amine moieties and so, regarded as the determinant of the success of the functionalization.

a) Fe@C-CONH-PEI conjugates (NANO-1.1-1.3)

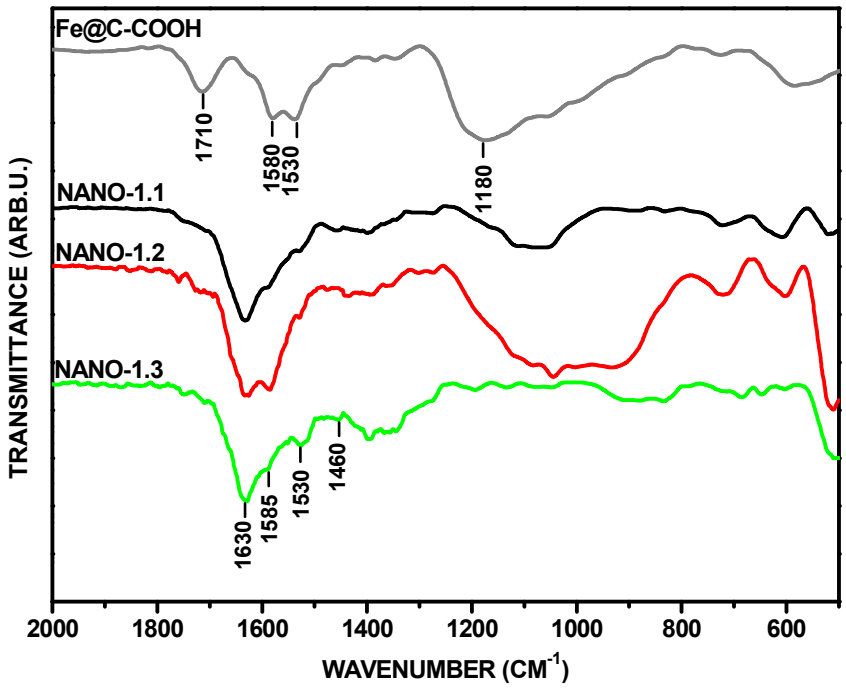

b) Fe@C-$(CH_2)_2$-CONH-PEI-pFBA conjugates (NANO-6.1-6.3)

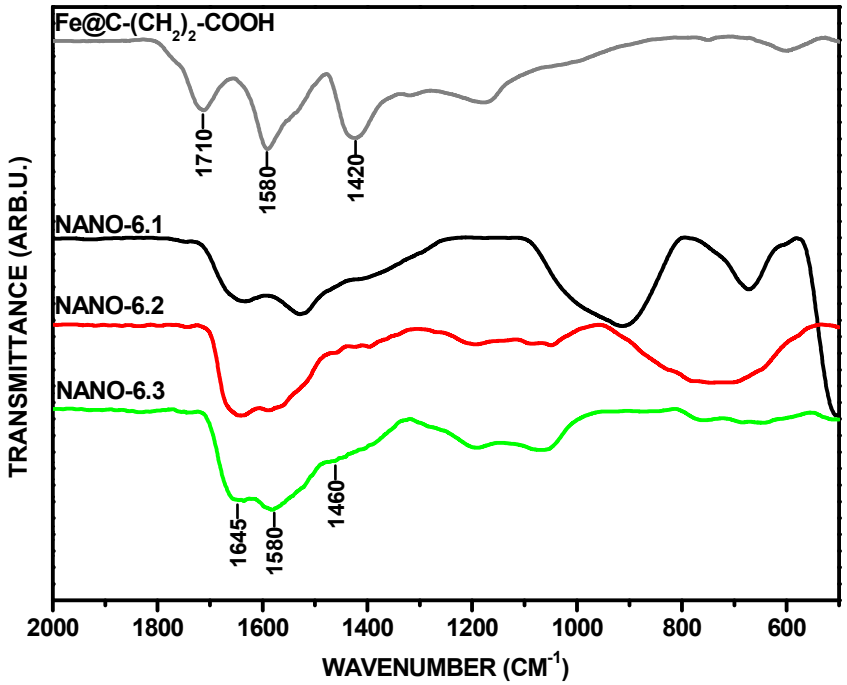

Fig. 8. FT-IR spectra of PEI-CEINs conjugates: **a**) NANO-1.1-1.3, **b**) NANO-6.1-6.3. See **Fig. 2** and **3** for legends

To evaluate the amount of the polymer conjugated to Fe@C-COOH and Fe@C-$(CH_2)_2$-COOH, thermogravimetric analysis (TGA) were carried out. Firstly, the TGA curves of PEI of different molecular weight were analyzed (Fig. S6 in Supplementary Data). The first weight loss, between c.a. 60 °C – 120 °C, is related to the presence of moisture. Further weight loss starts at c.a. 210 °C and is accompanied by the total decomposition of the polymer (without formation of the char). As we reported earlier for the surface-modified CEINs, under inert atmosphere the weight loss in range between 200 °C and 500 °C, was found to be 3.5% and 5.1% for Fe@C-COOH and Fe@C-$(CH_2)_2$-COOH, respectively.[31] Under nitrogen atmosphere, the magnetic core and the carbon coating, do not undergo degradation (except range above 500 °C, due to trace amounts of oxygen resulting in the oxidation of the carbon phase). In **Fig. 9** and **10**, the thermogravimetric curves of two representative conjugate lines are presented: Fe@C-CONH-PEI (NANO-1.1-1.3; **Fig. 9**) and Fe@C-$(CH_2)_2$-CONH-PEI-pFBA (NANO-6.1-6.3; **Fig. 10**) (for other TGA curves, please see graph 1-4 in Fig. S7 in Supplementary Data). A two-step decomposition is observed for the obtained conjugates. The first weight loss of c.a. 2-3 % in the temperature range between 60 °C – 120 °C, is due to the presence of moisture. The further weight loss starts at c.a. 200 °C and is completed at c.a. 530 °C. The weight loss for each conjugate is incomparably greater than for the pristine CEINs, which evidently indicates that the polymer was attached to surface-modified CEINs. Moreover, our studies showed, that due to the covalent attachment of PEI onto CEINs, the polymer do not undergo total decomposition at c.a. 375 °C, but at a higher temperature (compare representative DTG curves, in Fig. S8 in Supplementary Data). This weight change is between 12% and 60%, but this numbers cannot be directly taken as PEI content in samples, due to the weight loss in this temperature range for pristine CEINs with shorter or longer surface linker. Nevertheless, the PEI content (C_{PEI}) in each conjugate can be calculated according to the equation: $C_{PEI} = (W - M - L) \cdot 100\%$, where: W – observed weight loss for each conjugate, M – moisture, L – weight loss for linker on the surface on appropriate CEINs. However, L factor cannot be directly taken as the value for 'PEI-free' Fe@C-COOH and Fe@C-$(CH_2)_2$-COOH, due to the fact, that carbon materials are covalently-composed of the polymer and the nanoparticles. We have assumed, that the L factor can be approximated as follows: $L = LP_{nano} \cdot F_{CEINs}$, where LP_{nano} – the appropriate value for pristine linker-modified CEINs (3.5% or 5.1%), F_{CEINs} [%] – approximated relative fraction of CEINs in the carbon material, which was found to be between 50% and 88% (for the calculation method, please see Section IV in Supplementary Data). C_{PEI} (in other words, the conjugation yield) values are shown in **Table 1**. The PEI content was found to be between

6.5% and 52.4%. The highest conjugation yield is found for PEI 750kDa and its derivatives, especially for Fe@C-CONH-PEI750k-SA (C_{PEI} = 52.4%). The PEI content for CEINs conjugated with the pristine polymer, is ca. 1.64-1.91 fold higher for CEINs with longer surface linker, in comparison to the shorter one. It can be explained, by the higher content and better accessibility of carboxylic moieties for the Fe@C-$(CH_2)_2$-COOH material. Moreover, the conjugation yield is larger for the polymer of higher molecular weight, due to the increasing number of mer units in the polymer structure. Please note, that for the conjugates containing pre-modified PEI, the relations described above are not always fulfilled, i.e. for NANO-3.3 (52.4%) and NANO-4.3 (21.2%) and for NANO-5.3 (15.0%) and NANO-6.3 (11.%). Nevertheless, for most cases, using high molecular weight PEI and CEINs with longer surface linker, implied the higher content of PEI in the obtained carbon material. Thus, two main determinants of the conjugation process can be distinguished: the accessibility and content of: (i) primary amine groups of PEI and (ii) surface linker on the surface of CEINs. For PEI-SA and PEI-pFBA, the number of first-order amine moieties depends on the polymer pre-modification yield and it may not be related only to the molecular weight of PEI. Importantly, possible intramolecular electrostatic interactions between pre-introduced carboxylic functionalities (PEI-SA and PEI-pFBA) and amine groups in PEI structure, can significantly influence the conjugation process. If so, one has to consider the electrostatic effects and randomized, polymer-dependent process. For this kind of heterogeneous process, there is an appropriate set of parameters, which is related to accessibility of primary amine groups of PEI, PEI-SA, PEI-pFBA and the convenient orientation (accessibility) of surface-linker of CEINs and the reaction conditions.

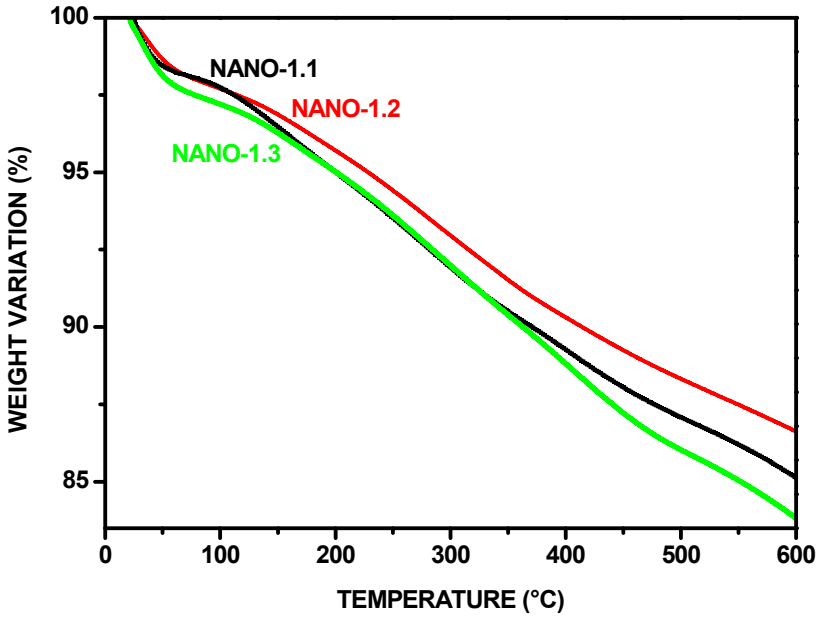

Fig. 9. TGA curves (in nitrogen) of Fe@C-CONH-PEI (NANO-1.1-1.3). See **Fig. 2** for legends

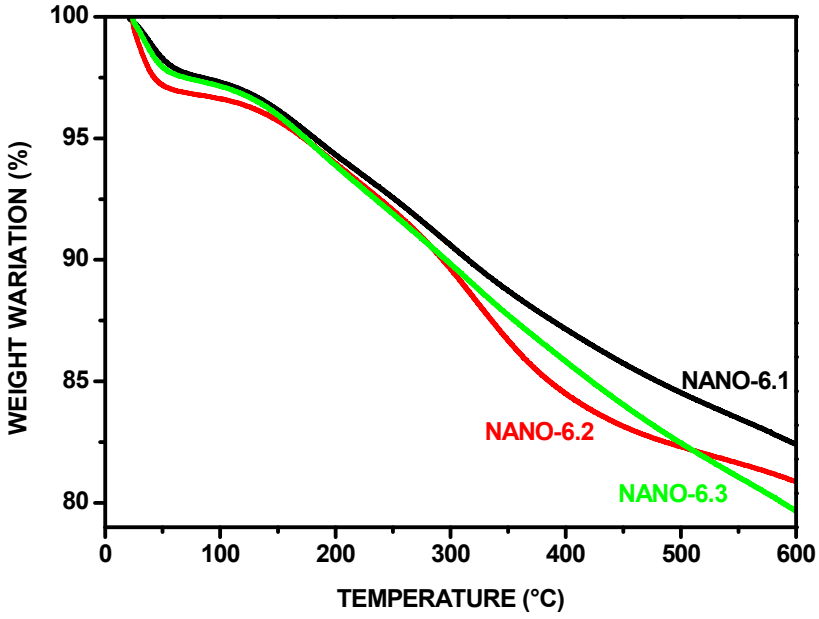

Fig. 10. Fe@C-$(CH_2)_2$-CONH-PEI-pFBA (NANO-6.1-6.3). See **Fig. 3** for legends

Table 1 -The content of PEI in obtained conjugates, evaluated from TGA

Structure	Content (%)	Structure	Content (%)
NANO-1.1 Fe@C-CONH-PEI0.8k	7.7	**NANO-2.1** Fe@C-$(CH_2)_2$-CONH-PEI0.8k	14.6
NANO-1.2 Fe@C-CONH-PEI25k	6.5	**NANO-2.2** Fe@C-$(CH_2)_2$-CONH-PEI25k	12.0
NANO-1.3 Fe@C-CONH-PEI750k	8.4	**NANO-2.3** Fe@C-$(CH_2)_2$-CONH-PEI750k	13.8
NANO-3.1 Fe@C-CONH-PEI0.8k-SA	7.0	**NANO-4.1** Fe@C-$(CH_2)_2$-CONH-PEI0.8k-SA	13.6
NANO-3.2 Fe@C-CONH-PEI25k-SA	21.8	**NANO-4.2** Fe@C-$(CH_2)_2$-CONH-PEI25k-SA	17.7
NANO-3.3 Fe@C-CONH-PEI750k-SA	52.4	**NANO-4.3** Fe@C-$(CH_2)_2$-CONH-PEI750k-SA	21.2
NANO-5.1 Fe@C-CONH-PEI0.8k-pFBA	6.7	**NANO-6.1** Fe@C-$(CH_2)_2$-CONH-PEI0.8k-pFBA	8.8
NANO-5.2 Fe@C-CONH-PEI25k-pFBA	6.8	**NANO-6.2** Fe@C-$(CH_2)_2$-CONH-PEI25k-pFBA	10.3
NANO-5.3 Fe@C-CONH-PEI750k-pFBA	15.0	**NANO-6.3** Fe@C-$(CH_2)_2$-CONH-PEI750k-pFBA	11.0

Transmission electron microscope (TEM) studies were carried out to finally confirm the presence of PEI on the CEINs surface and to analyze the morphology of conjugates. The representative microscopic images of the conjugates consisting shorter (**a**) and longer (**b**) surface linker are shown in **Fig. 11**. The surface functionalization of CEINs is clearly seen, in comparison to unmodified encapsulates (please compare with TEM images of CEINs, shown elsewhere[21,31]). The carbon encapsulate and its typical (graphitic) coating are surrounded by shapeless and inhomogeneous PEI layer. Also, basing on the TGA curves in oxygen (data not shown), the iron content in conjugates was found to be similar to the starting value for CEINs with shorter or longer surface linker. However those values are strictly connected with the polymer content in the conjugates.

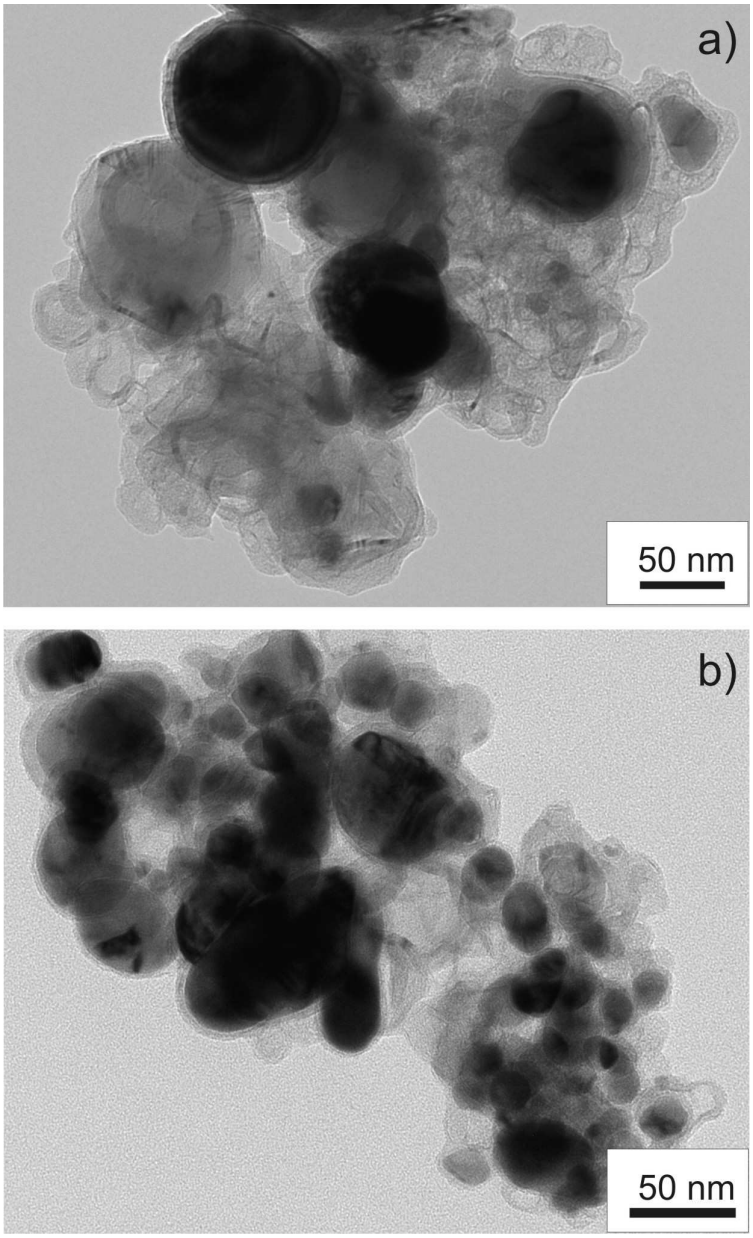

Fig. 11. Representative TEM images of: (**a**) NANO-1.3 and (**b**) NANO-2.2. See **Fig. 2** for legends

The samples of PEI25k-CEINs, as the representative conjugates, were suspended in water (100 μg·ml^{-1}) and subjected to dynamic light scattering (DLS) and zeta potential (ZP) measurements. The average particle size and surface zeta potential are listed in **Table 2**. The value of zeta potential for 4 of 5 samples is positive, due to the presence of cationic-type polymer. Unexpectedly, zeta potential of NANO-1.2 was found to be negative. This finding

may be correlated with the lowest polymer content in NANO-1.2, therefore high CEINs fraction in this conjugate (pristine surface-modified CEINs exhibit the negative zeta potential). However, there is a need for further detailed study to explain this phenomenon. The ZP was found to be lower for the structures containing pristine PEI in comparison to conjugates with pre-modified PEI. The values of ZP for NANO-3.2, NANO-4.2, NANO-5.2 and NANO 6.2 are higher than 30 mV and quite similar (30.-34.1 mV), which suggest well dispersion stability in water. The mean hydrodynamic particle size was found to be between 250 nm and 575 nm, and was 1.24-2.25 fold smaller for the conjugates comprising the longer surface linker (that is NANO-2.2, NANO-4.2 and NANO-6.2) in comparison to the shorter one. It is worth mentioning, that mean particle size (DLS measurements) for the pristine PEI 25kDa solution in water (100 $\mu g \cdot ml^{-1}$) was found to be 239 nm. The DLS and, especially, zeta potential measurements suggest the dispersion stability in the experimental media. Interestingly, the best dispersion stability in aqueous media was found to be the incredibly satisfactory for samples containing longer surface linkers. The carbon material containing the longer linker, pre-sonicated in water (100 $\mu g \cdot ml^{-1}$), remained in a stable dispersion form even for 60 days. This finding suggests, that the measured zeta potential is not a main determinant of the stability of obtained carbon material dispersion, but the length of the surface linker of CEINs. Please note, that this feature of carbon materials (and other drug-structures administered in the dispersion-form) is very important for the patient safety and the optimal therapeutic effect.

Table 2 - Surface zeta potential and the mean hydrodynamic particle size, measured by DLS [a]

Structure	Zeta potential [mV]	Size [nm]
NANO-1.2 Fe@C-CONH-PEI25k	-8.1	575
NANO-2.2 Fe@C-$(CH_2)_2$-CONH-PEI25k	+18.1	256
NANO-3.2 Fe@C-CONH-PEI25k-SA	+32.2	479
NANO-4.2 Fe@C-$(CH_2)_2$-CONH-PEI25k-SA	+32.2	383
NANO-5.2 Fe@C-CONH-PEI25k-pFBA	+30.1	378
NANO-6.2 Fe@C-$(CH_2)_2$-CONH-PEI25k-pFBA	+34.1	287

[a] carbon material samples were suspended in distilled water, concentration 100 μg/ml

3.3 Study on the physical adsorption of PEI onto CEINs

The review of recent literature leads to the conclusion that there are two different pathways of creating pre-nanotheranostic platforms: covalent immobilization of macromolecule onto surface-modified nanomaterial or non-covalent modification (physical adsorption). The EDCl-mediated approach is the most encountered synthetic strategy of covalent attachment of high-molecular weight molecules, i.e. proteins or cationic polymers, to surface-modified carbon nanomaterials.[60] However, there is still a high probability of non-covalent electrostatic adsorption of a biomolecule. Hence, it is very important to verify the possibility of non-covalent adsorption for each newly synthesized nanomaterial-biomolecule conjugate. Therefore, we have checked the probability of the adsorption of PEI 0.8 kDa and 25 kDa onto CEINs. The polymer and carbon-encapsulated iron nanoparticles: pristine (without linker) and surface-modified (with $(CH_2)_2COOH$ linker), were sonicated for 5 h. Then the suspensions were centrifuged several times in methanol and dried. The PEI content in the supernatants were monitored by TLC (a ninhydrin test was used). There was no weight gain in Fe@C sample, whilst weight gain of ca. 4 - 5% were

observed in Fe@C-$(CH_2)_2$-COOH samples. To confirm the supposition of PEI adsorption, thermogravimetric and spectroscopic (FT-IR) analyses were performed. There were no characteristic signals of PEI in the FT-IR spectra and any essential weight loss in the TGA curves for linker-free nanomaterial samples were observed. For both Fe@C-$(CH_2)_2$-COOH samples we have found characteristic features for surface-modified CEINs and PEI (please see Fig. S9 in Supplementary Data). The polymer content in each sample was ca. 10% wt. according to TGA. Therefore, we can conclude that PEI adsorption onto linker-modified CEINs is very strong, whereas polymer is not adsorbed onto unmodified CEINs.

In order to reduce the PEI-adsorption phenomena, while applying EDCl-NHS-mediated approach, per 1 mol COOH groups on the surface of the carbon material, we have been using 10 and 25 mol equivalent of EDCl and NHS, respectively. The carboxylic groups on CEINs surface were activated before PEI addition. What is worth noticing is that in the non-covalently modified structures the noticeable signal on infrared spectra at ca. 1740 cm^{-1} was observed (C=O stretching vibration in the carboxylic groups; please see Fig. S9 in Supplementary Data), whilst this band was absent in the covalently-synthesized structures This means that all carboxylic groups participate in the formation of covalent amide bonds while applying EDCl-NHS-mediated synthetic pathway. Further research on the non-covalent PEI attachment is currently underway.

4. Conclusions

The modification of polyethylenimine and conjugation to carbon-encapsulated iron nanoparticles was presented. Firstly, the PEI derivatives were synthesized by two synthetic strategies: (i) amide-type reaction using succinic acid anhydride (PEI-SA) and (ii) reductive amination using *p*-formylbenzoic acid (PEI-pFBA). The reaction yield was found to be between ca. 50-57%. NH_2 : NH : N ratio value for PEI 25kDa products is 1 : 1.62 : 1.32 and 1 : 1.69 : 1.39, for PEI25k-SA and PEI25k-pFBA, respectively (the ratio for pristine PEI 25kDa 1 : 1,12 : 0.89). Those values show, that carboxylic functionalities were successfully introduced onto PEI surface. The structure of the polymer derivatives were analyzed using spectroscopic methods (NMR, FT-IR). Moreover, the measured zeta potential of PEI 25kDa and its derivatives suggested, that obtained modification level (the amount of introduced functionalities) does not significantly reduce the PEI capability to bind other biomolecules and should provide lower toxicity of polymer. Next, PEI and its derivatives were conjugated with CEINs containing shorter or longer surface linker, by carbodiimide-amine type reaction

between primary amino moieties of PEI and carboxylic functionalities onto magnetic nanoparticles. The success of the conjugation was confirmed by FT-IR spectroscopy, thermogravimetry and transmission electron microscopy. The PEI amount in conjugates was between 6.50% and 52.36%. In most cases, higher polymer content in the conjugate was found for CEINs with longer surface linker and PEI of high molecular weight. Moreover, the obtained conjugates did not contain 'free' carboxylic moieties onto CEINs surface. A very good dispersion stability in aqueous media was found for samples containing the longer surface linker. Finally, the non-covalent adsorption phenomena was investigated. Strong electrostatic interactions between PEI amino moieties and carboxylic moieties onto carbon encapsulates were observed, whilst PEI adsorption was not observed onto pristine ('linker-free') CEINs. We claim, that the possibility of PEI adsorption, while using covalent-type conjugation technique, was reduced to the absolute minimum by using a large excess of coupling reagents and an appropriate synthetic procedure. In overall conclusion, our study sheds a new light onto the conjugation technique of PEI and its derivatives to the promising nanocarrier and drug-contrast candidate – carbon-encapsulated iron nanoparticles. Both PEIs and CEINs offer some interesting and theranostic features, so its potential conjugates can be very useful i.e. in MRI-based molecular diagnostics and targeted anticancer therapies.

Acknowledgments

This work was financially supported partially by Warsaw University of Technology and GEMNS project granted in the European Union's Seventh Framework Programme under frame of the ERA-NET EuroNanoMed II (European Innovative Research and Technological Development Projects in Nanomedicine).

References

1. H. van den Berg, J. N. van den Anker and J. H. Beijnen, *Cancer Treat. Rev.*, 2012, **38**, 3-26.
2. E. Chatelut, J. P. Delord and P. Canal, *Invest. New Drugs.,* 2003, **21**, 141-148.
3. N. Hedhli and K. S. Russell, *Curr. Hypertens. Rep*., 2010, **12**, 411–417.

4. Y. Li, T. Lin, Y. Luo, Q. Liu, W. Xiao, W. Guo, D. Lac, H. Zhang, C. Feng, S. Wachsmann-Hogiu, J.H. Walton, S. R. Cherry, D. J. Rowland, D. Kukis, C. Pan and K. S. Lam, *Nat. Commun.*, 2014, **5**, art. no. 4712.
5. T. Lammers, F. Kiessling, W. E. Hennink and G. Storm, *J. Control. Release*, 2012, **161**, 175–187.
6. E. K. Lim, T. Kim, S. Paik, S. Haam, Y. M. Huh and K. Lee, *Chem. Rev.*, 2015, **115**, 327–394.
7. D. Peer, J. M. Karp, S. Hong, O. C. Farokhazad, R. Margalit and R. Langer, *Nat. Nanotech.*, 2007, **2**, 751–760.
8. F. Valentini, M. Carbone and G. Palleshi, *Anal. Bioanal. Chem.*, 2013, **405**, 451–465.
9. Z. Fan , P. P. Fu, H. Yu and P. C. Ray, *J. Food Drug Anal*., 2014, **22**, 3-17.
10. M. S. Muthu, D. T. Leong, L. Mei and S. S. Feng, *Theranostics*, 2014, **4**, 660-677.
11. T. Moore, H. Chen, R. Morrison, F. Wang, J. N. Anker and F. Alexis, *Mol. Pharm.*, 2014, **11**, 24–39.
12. M. Das, S. R. Datir, R. P. Singh and S. Jain, *Mol. Pharm.*, 2013, **10**, 2543−2557.
13. S. Mura and P. Couvreur, *Adv. Drug Deliv. Rev.,* 2012, **64**, 1394–1416.
14. Z. P. Xu, Q. H. Zengb, G. Q. Lua and A. B. Yub, *Chem. Eng. Sci.*, 2006, **61**, 1027–1040.
15. M. Orecchioni, R. Cabizza, A. Bianco and L. G. Delogu, Theranostics, 2015, **5**, 710-723.
16. S. Afreen, K. Muthoosamy, S. Manickam and U. Hashim, *Biosens. Bioelectron.*, 2015, **63**, 354–364.
17. S. Bosi, T. Da Ros, G. Spalluto and M. Prato, *Eur. J. Med. Chem.,* 2003, **38**, 913-923.
18. J. Borysiuk, A. Grabias, J. Szczytko, M. Bystrzejewski, A. Twardowski and H. Lange, *Carbon*, 2008, **46**, 1693-1701.
19. M. Bystrzejewski, A. Huczko and H. Lange, *Sens. Actuar. B*, 2005, **109**, 81–85.
20. I. P. Grudzinski, M. Bystrzejewski, M. A. Cywinska, A. Kosmider, M. Poplawska, A. Cieszanowski, Z. Fijalek and A. Ostrowska, *Colloids Surf., B*, 2014, **117**, 135–143.
21. I. P. Grudzinski, M. Bystrzejewski, M. A. Cywilska, A. Kosmider, M. Poplawska, A. Cieszanowski and A. Ostrowska, *J. Nanopart Res.*, 2013, **15**, 1835.
22. I. P. Grudzinski, M. Bystrzejewski, M. A. Cywinska, A. Kosmider, M. Poplawska, A. Cieszanowski, Z. Fijalek, A. Ostrowska and A. Parzonko, *J. Appl. Toxicol.,* 2014, **34**, 380–394.
23. B. Behnam, W. T. Shier, A. H. Nia, K. Abnous and M. Ramezani, *Int. J. Pharm*., 2013, **454**, 204–215.

24. S. Polizu, O. Savadogo, P. Poulin and L. Yahia, *J. Nanosci. Nanotechnol.,* 2006, **6**, 1883-1904.
25. Z. Liu, X. Sun, N. Nakayama-Ratchford and H. Dai, *ACS Nano*, 2007, **1**, 55–56.
26. H. Ali-Boucetta, K. T. Al-Jamal, D. McCarthy, M. Prato, A. Bianco and K. Kostarelos, *Chem. Commun.*, 2008, 459-461.
27. C. Klumpp, K. Kostarelos, M. Prato and Alberto Bianco, *Biochim. Biophys. Acta*, 2006, **1758**, 404–412.
28. S. W. Kim, T. Kim, Y. S. Kim, H. S. Choi, H. J. Lim, S. J. Yang and C. R. Park, *Carbon*, 2012, **50**, 3-33.
29. S. Eigler and A. Hirsch, *Angew. Chem. Int. Ed.,* 2014, **53**, 2 – 21.
30. M. Quintana, E. Vazquez and M. Prato, *Acc. Chem. Res.*, 2013, **46**, 138–148.
31. M. Poplawska, M. Bystrzejewski, I. P. Grudzinski, M. A. Cywinska, J. Ostapko and A. Cieszanowski, *Carbon*, 2014, **74**, 180-194.
32. M. Popławska, G. Z. Zukowska, S. Cudziło and M. Bystrzejewski, *Carbon*, 2010, **48**, 1312-1320.
33. S. K. Samal, M. Dash, S. Van Vlierberghe, D. L. Kaplan, E. Chiellini, C. van Blitterswijk, L. Moronid and P. Dubruel, *Chem. Soc. Rev.*, 2012, **41**, 7147-7194.
34. R. Soleyman and M. Adeli, *Polym. Chem.*, 2015, **6**, 10-24.
35. O. M. Merkel, D. Librizzi, A. Pfestroff, T. Schurrat, K. Buyens, N. N. Sanders, S. C. De Smedt, M. Béhé and T. Kissel, *J. Control. Release*, 2009, **138**, 148–159.
36. H. Ragelle, G. Vandermeulen and V. Préat, *J. Control. Release*, 2013, **172**, 207-218.
37. A. F. M. El-Mahdy, T. Shibata, T. Kabashima, Q. Zhu and M. Kai, *RSC Adv.*, 2015, **5**, 32775–32785.
38. S. A. Meenach, Y. J. Kim, K. J. Kauffman, N. Kanthamneni, E. M. Bachelder and K. M. Ainslie, *Mol. Pharm.*, 2012, **9**, 290−298.
39. J. Zhao, C. Lu, X. He, X. Zhang, W. Zhang and X. Zhang, *ACS Appl. Mater. Interfaces*, 2015, **7**, 2607–2615.
40. H. Wu, H. Shi, H. Zhang, X. Wang, Y. Yang, C. Yu, C. Hao, J. Du, H. Hu and S. Yang, *Biomaterials*, 2014, **35**, 5369-5380.
41. M. Shen, S. H. Wang, X. Shi, X. Chen, Q. Huang, E. J. Petersen, R. A. Pinto, J. R. Baker Jr. and W. J. Weber Jr., *J. Phys. Chem. C*, 2009, **113***,* 3150–3156.
42. S. Foillard, G. Zuber and E. Doris, *Nanoscale*, 2011, **3**, 1461-1464.
43. M. Zhang, Y. Li, Z. Su and G. Wei, *Polym. Chem.*, 2015, **6**, 6107-6124.

44. L. Feng , X. Yang , X. Shi, X. Fan, R. Peng, J. Wang and Z. Liu, *Small*, 2013, **9**, 1989-1997.
45. G. Wei, R. Dong, D. Wang, L. Feng, S. Dong, A. Song and J. Hao, *New J. Chem*., 2014, **38**, 140-145.
46. L. Feng, S. Zhang and Z. Liu, *Nanoscale*, 2011, **3**, 1252–1257.
47. A. Zintchenko, A. Philipp, A. Dehshahri and E. Wagner, *Bioconjugate Chem.*, 2008, **19**, 1448–1455.
48. S. Nimesh A. Aggarwal, P. Kumar, Y. Singh, K. C. Gupta and R. Chandra, *Int. J. Pharm.,* 2007, **337**, 265–274.
49. P. Y. Teo, C. Yang, J. L. Hedrick, A. C. Engler, D. J. Coady, S. Ghaem-Maghami, A. J. T. George and Y. Y. Yang, *Biomaterials*, 2013, **34**, 7971-7979.
50. X. Chen, Z. Yuan, X. Yi, R. Zhuo and F. Li *Nanotechnology*, 2012, **23**, 415602.
51. X. Zhang, Y. Duan, D. Wang and F. Bian, *Carbohydr. Polym.*, 2015, **122**, 53–59.
52. W. Tseng, and C. Jong, *Biomacromolecules*, 2003, **4**, 1277-1284.
53. J. Wang, B. Dou and Y. Bao, *Mater. Sci. Eng. C*, 2014, **34**, 98–109.
54. S. Wen, F. Zheng, M. Shen and X. Shi., *J. Appl. Polym. Sci.*, 2013, **128**, 3807–3813.
55. H. Petersen, P. M. Fechner, D. Fischer and T. Kissel, *Macromolecules*, 2002, **35**, 6867-6874.
56. K. S. Siu, D. Chen, X. Zheng, X. Zhang, N. Johnston, Y. Liu, K. Yuan, J. Koropatnick, E. R. Gilles and W.-P. Min, *Biomaterials*, 2014, **35**, 3435-3442.
57. X. Cao, Z. Li, X. Song, X. Cui, P. Cao, H. Liu, F. Cheng and Y. Chen, *Eu. Polym. J.,* 2008, **44**, 1060–1070.
58. H. Liu, Z. Shen, S.-E. Stiriba, Y. Chen, W. Zhang and L. Wei, *J. Polym. Sci. A Polym. Chem*., 2006, **44**, 4165-4173.
59. H. Lv, S. Zhang, B. Wang, S. Cui and J. Yan, *J. Contr. Release,* 2006, **114**, 100–109.
60. Y. Gao and I. Kyratzis, *Bioconjugate Chem*., 2008, **19**, 1945–1950.